ACADEMIC PRESS

Available online at www.sciencedirect.com

SCIENCE DIRECT®

DEVELOPMENTAL BIOLOGY

Developmental Biology 258 (2003) 277–290

www.elsevier.com/locate/ydbio

# Development of a rod photoreceptor mosaic revealed in transgenic zebrafish

James M. Fadool*

*Department of Biological Science, The Florida State University, Tallahassee, FL 32306-4340, USA*

Received for publication 11 September 2002, revised 23 January 2003, accepted 18 February 2003

**Abstract**

The number and distribution of neurons within the vertebrate retina are tightly regulated. This is particularly apparent in the highly ordered, crystalline-like arrangement of the cone photoreceptors in the teleost. In this report, using a transgenic line of zebrafish, a novel and developmentally regulated mosaic pattern of the rod photoreceptors is described. The spatial and temporal expression of EGFP, under the control of the *Xenopus* rhodopsin gene promoter, was nearly identical to the endogenous rhodopsin. EGFP was first detected in the ventral nasal retinal in an area of precocious neurogenesis referred to as the "ventral patch". Subsequent expression of EGFP was observed in isolated cells sporadically distributed across the dorsal and central retina. However, confocal microscopy and spatial analysis of larval eyes or retinal explants from adults revealed a precise arrangement to the rod photoreceptors. The rod terminals were arranged in regularly spaced rows with clearly identifiable telodendria linking neighboring cells. The rod inner segments projected through the cone mosaic in a predictable pattern. In the adult, the rod mosaic originated near the retinal margin where clusters of rods differentiated around the immature short single cone. In the embryo, the sporadic differentiation of the rods led to the gradual formation of the mosaic pattern. With the growing interest in neuronal stem cells, revisiting this model of neurogenesis provides an avenue to uncover mechanisms underlying the precise integration of new neuronal elements into a preexisting neural network.


*Keywords:* Rod photoreceptor; Retina; Development; Mosaic; Transgenic; Zebrafish

## Introduction

The elegant organization of the vertebrate neural retina into three distinct cellular layers and two synaptic layers has made it a tractable model to investigate physiological processes as well as developmental mechanisms of the central nervous system (Livesey and Cepko, 2001; Masland and Raviola, 2000; Masland, 2001). The well-characterized, laminar organization of the retina is complemented by the nonrandom or mosaic organization of the neuronal populations within each of the layers (Cook and Chalupa, 2000; Wassle and Riemann, 1978). The necessity of the uniform distribution of cells for uniform light gathering and parallel processing should be readily apparent. Gaps in the distribution of cells or random clustering would result in under-representation or over-sampling of information in those regions of the visual field.

It was somewhat unexpected to find that the mosaic arrangements of different cell types were random with respect to one another (Cameron and Carney, 2000; Rockhill et al., 2000; Wassle et al., 1981). For example, in the mouse retina, the distribution of horizontal cells was independent of the distribution of A2 amacrine cells. Likewise, the distribution of starburst amacrine cells located in the inner nuclear layer was random relative to the distribution of displaced starburst amacrine cells that reside in the ganglion cell layer. Similarly, in the zebrafish, the positions of the somatostasin-containing neurons were random with respect to the tyrosine hydroxylase-positive neurons. The anatomical data in conjunction with computer modeling and recent experimental evidence suggest that homotypic cell interactions could initially account for the regular spacing of cells within the retina (Galli-Resta, 2000; Stenkamp and Cam-

* Fax: +1-850-644-0989.
*E-mail address:* jfadool@bio.fsu.edu (J.M. Fadool).

0012-1606/03/$ – see front matter © 2003 Elsevier Science (USA). All rights reserved.
doi:10.1016/S0012-1606(03)00125-8

eron, 2002). Subsequently, tangential dispersion of newly postmitotic cells and rearrangement of cells within the mosaic could contribute significantly to the maintenance of the regular spacing (Reese and Galli-Resta, 2002; Reese et al., 1995). Lastly, local interactions between dendritic processes act to refine the local architecture and synaptic connections (Lohmann and Wong, 2001).

One notable exception to the random patterning of different neuronal types within the retina is the interdependence of cone arrangements in the teleost retina (Ali, 1976; Ali et al., 1978; Engstrom, 1960; Stenkamp et al., 2001). In most vertebrates, two types of photoreceptor have evolved: the rods, which mediate dim light vision, and the cones, that detect light of much greater intensity, with a faster temporal resolution and convey color specific information (Kolb et al., 2001). The cones of fishes can be readily distinguished by morphology, opsin expression, and spectral characteristics. Moreover, the position of each cone subtype is precisely arranged relative to the others (Ali, 1976). The result is a highly ordered, crystalline-like mosaic. For example, the retina of the zebrafish contains four distinct retinal cones: short single cones sensitive to ultraviolet light, long single cones sensitive to blue light, and double cones comprised of a red-sensitive and a green-sensitive member (Engstrom, 1960; Raymond et al., 1993; Vihtelic et al., 1999). The mosaic is composed of rows of alternating blue- and UV-sensitive single cones that alternate in turn with rows of red- and green-sensitive double cones. The parallel rows are aligned such that the green-sensitive members of the double cones flank the short single cones, and the long single cones are nearer to the red-sensitive member of the double cone.

Based on the temporal and spatial sequence of cone opsin expression, it was proposed that local cell–cell interactions underlie the pattern of cone differentiation (Stenkamp and Cameron, 2002). In zebrafish larvae and the closely related goldfish, opsin expression is first detected in the ventral patch, the site of precocious neurogenesis in the ventral–nasal retina (Hu and Easter, 1999). The red-sensitive opsin was first detected, followed by blue or green, and lastly the UV-sensitive opsin (Raymond et al., 1995; Stenkamp et al., 1996, 1997). Following the initial appearance in the ventral patch, opsin expression progressed in a wave-like fashion across the nasal, dorsal, and temporal regions. In the zebrafish, the presence of a cone mosaic was demonstrated in the ventral retina 54 h postfertilization (hpf), although regular spacing of the cells suggested that it was present prior to this time (Larison and BreMiller, 1990).

In addition to cones, the zebrafish retina also contains an abundance of densely packed rod photoreceptors. The rod cell bodies are located vitread to the cone nuclei, and in the light-adapted retina, the thin rod inner and outer segments project beyond the cones to interdigitate with the apical microvilli of the pigmented epithelium. In the zebrafish, differentiation of rods follows a developmental program distinct from that of the cones. Rhodopsin was initially detected in the ventral patch, preceding the expression of the cone opsins. However, in the dorsal and central retina, sporadically distributed cells expressed rhodopsin after the differentiation of the cones (Raymond et al., 1995; Schmitt and Dowling, 1996).

The study of neurogenesis in teleosts offers several distinct advantages over other models. Most teleosts continue to grow throughout their life, and this increase in body mass is matched by a proportionate increase in the size of the eye and area of the retina (Fernald, 1990). The increased retinal area is achieved through two distinct mechanisms. First, new neurons, including cones, are generated from a population of mitotic progenitor cells located at the retinal margin. Second, the retina is gradually stretched within the eyecup with a comparable thinning of the retinal layers and increased spacing between the nuclei. Visual acuity is preserved by the increased size of the retinal image in proportion to the growth of the eye (Fernald, 1990). However, to compensate for the greater area of the retina and maintain visual sensitivity, rods are inserted into the photoreceptor cell layer near the margin and across the retina from a distinct population of mitotic progenitor cells located in the inner nuclear layer (Hagedorn and Fernald, 1992; Johns and Fernald, 1981; Julian et al, 1998; Marcus et al, 1999; Ottenson et al., 2002). In the zebrafish, the sporadic maturation of rods in the larval retina and the uneven mitosis of rod progenitors across the adult retina contributed to the conclusion that the rods were not arranged in a mosaic.

In this report, data are presented that challenge this notion of sporadic differentiation and random packing of rod photoreceptor cells in the zebrafish retina. In a transgenic line of zebrafish, green fluorescent protein (EGFP) under the control of the 5′ upstream fragment from the *Xenopus* rhodopsin gene demonstrated spatial and temporal expression nearly identical to the endogenous opsin. Unexpectedly, the expression of EGFP revealed the first example of the development of a rod mosaic in the larvae and adult zebrafish. The overall similarities in the mosaic patterns of the larva and adult suggested a similar developmental mechanism, while the observed differences may be due to the rate of rod genesis.

## Materials and methods

### *Maintenance of fish*

Rearing, breeding, and staging of zebrafish were performed as described (Fadool et al., 1997). Inbred zebrafish derived from stocks originally obtained from Ekkwill fish farm (Clearwater, FL) and *albino*$^{b4}$ fish (University of Oregon) were used throughout the study.

*Plasmids*

The XopsEGFP-N1 plasmid was provided by David Papermaster and Orson Moritz. This contains 5.5 kb of genomic DNA upstream of the 5′-initiation sequence of the *Xenopus* rhodopsin gene driving the expression of the EGFP (Knox et al., 1998; Moritz et al., 1999). In transient assays, this was sufficient for rod-specific expression of EGFP in zebrafish embryos.

Plasmids containing the cDNAs for the zebrafish rhodopsin and cone opsins were provided by Thomas Vihtelic and David Hyde (Vihtelic et al., 1999). For in situ hybridization, the EGFP sequence from pEGFP-N1 (Clonetech) was amplified by PCR and blunt-end ligated into the *Eco*RV site of pSTBlue (Novagen).

*Generation of transgenic fish*

Plasmid DNA was purified by using a commercial miniprep kit (Bio-Rad) and eluted in water. One- and two-cell stage zebrafish embryos from pairwise matings were microinjected with ~1 nl of solution containing the plasmid DNA at a concentration of 25 μg/ml. Surviving embryos were reared to adulthood and mated. Beginning at 24 hpf, $F_1$ progeny were screened for expression of the reporter gene. Briefly, three to four embryos were sorted into each well of thin-bottom, 96-well plates. EGFP fluorescence was viewed under a Zeiss Axiovert 100 microscope outfitted with epifluorescence and a 2.5× Fluar objective lens. Five percent of the $F_1$ embryos from a single founder expressed EGFP. The $F_1$ offspring were grown to breeding stage and outcrossed to noninjected Ekkwill fish. Transgenic animals were also mated to fish homozygous for the *albino*$^{b4}$ mutation. The resulting transgenic, pigmented fish were inbred, and the resulting, nonpigmented larvae demonstrating retinal-specific EGFP expression were used for image analysis.

*Whole-mount in situ hybridization*

RNA in situ hybridization was performed essentially as described (Hyatt et al., 1996) by using DIG-labeled riboprobes and alkaline phosphatase-conjugated Fab fragments according to the manufacturer's recommendations (Roche). For double labeling, a second riboprobe incorporating FITC-UTP was detected by using peroxidase-conjugated anti-FITC antibodies and DAB as substrate as suggested (Roche). Hybridization with two probes was conducted simultaneously, and immunolabeling and detection with peroxidase and alkaline phosphatase-conjugated secondary antibodies were conducted sequentially. The embryos were cleared in a graded series of glycerol. The eyes were removed from the larvae prior to microscopic analysis.

*Immunofluorescence and histology*

Eyes were dissected from adult zebrafish, and retinas were fixed in 4% paraformaldehyde in 80% Hank's balanced salt solution at 4°C for 4 h to overnight. Tissues were rinsed in buffer and cryoprotected in 30% sucrose solution. Tissues were mounted in several different orientations in OCT medium (Miles Scientific) and frozen on dry ice. Sections, 7–10 μm in thickness, were adhered to gelatin-coated glass slides and stored at −20°C. Prior to immunolabeling, sections were postfixed in 2% paraformaldehyde. Immunofluorescent labeling using polyclonal antiserum against the cone opsins (Vihtelic et al., 1999) or the 1D1 monoclonal antibody (Hyatt et al., 1996) that recognizes an epitope on rhodopsin, in combination with species-specific Texas Red- or Cy3-conjugated secondary antibodies (Jackson Labs), were essentially as described (Peterson et al., 2001). Sections were counterstained with DAPI (4′, 6-diamidino-2-phenylindole; Sigma). Tissues were viewed on the Zeiss Axiovert microscope, and images were captured and processed by using the Zeiss Axiocam Digital Camera and Axiovision software.

For histological analysis, larvae were fixed with 1% gluteraldehyde and 1% osmium tetroxide in 0.1 M cacodylate buffer and processed as previously described (Fadool et al., 1997). Plastic sections were stained with a solution of 1% methylene blue in 1% borax.

*Confocal imaging*

Adult zebrafish were either dark adapted for several hours or used prior to lights on in the morning. All procedures were conducted under dim red light. Animals were anesthetized with tricaine and decapitated. Eyes were removed, being careful to cut the optic nerve just proximal to the sclera to minimize distortion of the retina. Following removal of the cornea and lens, the sclera was gently torn with forceps, and the retina, without the adherent pigmented epithelium, was removed from the eyecup and placed in teleost saline supplemented with glucose and 10 mM sodium bicarbonate. For confocal microscopy, several slits were cut at the retinal margin, and the retinas were mounted flat between two coverslips separated by the thickness of one No. 1 coverslips and sealed with silicone grease. In this fashion, retinas could be imaged from either the ganglion cell or photoreceptor cell surface.

To facilitate imaging of EGFP at earlier stages of development, the transgenic *albino* embryos and larvae were anesthetized and mounted between glass coverslips in 0.5% agarose in 10% Hank's solution. For larvae between 4 and 21 dpf, following anesthesia, the eyes were removed by using glass or tungsten needles. For specimen older than 8 dpf, the retina and pigmented epithelium were dissected away from the sclera, choroid, and lens. Larval eyes and

retinas were mounted between glass coverslips separated by thin strips of mica and sealed with silicone.

Images were captured at a resolution of 1024 × 1024 pixels by using a Zeiss 510 Scanning Laser Confocal microscope equipped using either a 20× (NA 0.75) objective or 40× water immersion (NA 1.2) objective. The laser was operated between 0.5 and 5% output. For presentation, images were processed by using LSM510 software or Metamorph (Universal Imaging) prior to export to Photoshop (Adobe).

*Quantitative analysis*

The arrangements of cells in optical sections taken from confocal images were subjected to pattern analysis. To compensate for unevenness of the flat mounts, neighboring regions taken from optical sections were assembled by using the tiling function in Metamorph. The functions of the LSM510 software were used to compensate for tilting of the eye preparations. Accuracy of the manipulations was verified by using the transparency function in Powerpoint to overlay the original and the newly generated images and visually inspecting that neighboring points remained in register. To test for regularity of the rod mosaic, the EGFP fluorescent structures in digital images were assigned *(x,y)* coordinates in Scion Image Software (Scion). For each point in the field, the nearest neighbor distance (NND) was determined by using Biotas (Version 1.02; Ecological Software Solutions), and the spread sheet was exported to Excel (Microsoft) to calculate the mean NND and standard deviation (SD) for all points in the field. For each sample, the conformity ratio (CR) was calculated as the NND divided by the SD and analyzed for nonrandomness using the Ready-Reckoner Chart of Cook (1996).

## Results

*Generation of transgenic zebrafish*

In preliminary studies, expression vectors containing 5.5 kb, 1.2 kb, and 508 bases of 5′-upstream sequence of the Xenopus rhodopsin promoter and the EGFP reporter gene were injected into one- to two-cell-stage zebrafish embryos. Although transient expression of EGFP was observed with each construct, the intensity, onset, and distribution of expression observed for the 5.5-kb promoter most closely matched that of the reported distribution of rhodopsin (Raymond et al., 1995; Schmitt and Dowling, 1996); therefore, embryos injected with this construct were grown to adults for subsequent analysis.

Founder fish injected with the 5.5-kb XOPS-EGFP plasmid were pairwise mated, and the $F_1$ progeny were screened for retinal-specific expression of EGFP. From 18 successful matings, a single female was identified that transmitted the transgene to 5% of the $F_1$ generation. The 5% inheritance frequency demonstrated mosaicism of the germ line. Transgenic $F_1$ fish were raised to adults and outcrosses to uninjected fish. From these matings, approximately 50% of the $F_2$ progeny expressed the reporter gene demonstrating a Mendelian pattern of inheritance. To facilitate observation of EGFP expression in living animals, the transgene was crossed into a line of zebrafish carrying the *albino* mutation. Transgenic, homozygous *albino* larvae were identified in subsequent generations. The use of nonpigmented animals resulted in less variability in the onset of expression of EGFP compared with PTU treatment. No differences in onset of reporter gene expression were observed between normally pigmented and *albino* larvae.

*Developmental distribution*

In the majority of the transgenic embryos, the fluorescence of EGFP was first detected between 55 and 58 hpf in a single cell or cluster of three or five cells located in the ventral–nasal retina. The intensity and distribution of fluorescence dramatically increased between 60 and 72 hpf. By 60 hpf, the patch of EGFP consists of several rows containing two to five photoreceptors each (Fig. 1A). By 72 hpf, EGFP was observed in numerous cells within the ventral–nasal retina and had spread to the temporal side of the choroid fissure. By 84 hpf, fluorescence was observed by individual cells sporadically distributed across the central and dorsal retina (Fig. 1C).

The cellular specificity and timetable of EGFP transcription were compared with that of the endogenous opsin by in situ hybridization (Fig. 1D–F). The first opsin transcript could be detected at 50–52 hpf compared with 55 hpf for EGFP. At 72 hpf, both transcripts were observed in a patch of cells in the photoreceptor cell layer in the ventral nasal retina with occasional labeling of cells on the temporal side of the choroid fissure (Fig. 1D). By 96 hpf, expression had spread to the dorsal and central retina. Double-labeling in situ hybridization for both the rod opsin and EGFP demonstrated that all cells labeled for the EGFP transcript were colabeled for rod opsin transcript (Fig. 1F). The only minor difference in expression between the two was that, at all stages examined, the distribution of the EGFP label was slightly delayed or restricted relative to the endogenous gene (Fig. 1D and E). The delay was estimated to be on the order of a few hours, as the range of labeling for EGFP or rhodopsin within a single clutch demonstrated considerable overlap.

In addition to the retina-specific expression, approximately 75% of the transgenic embryos demonstrated EGFP fluorescence in the pineal (Fig. 1B). The pineal is located in the midline, dorsal to the diencephalon. Consistent with the reporter gene expression, the photoreceptor cells of the pineal labeled for the rod opsin transcript or protein by in situ hybridization or immunochemistry (data not shown).

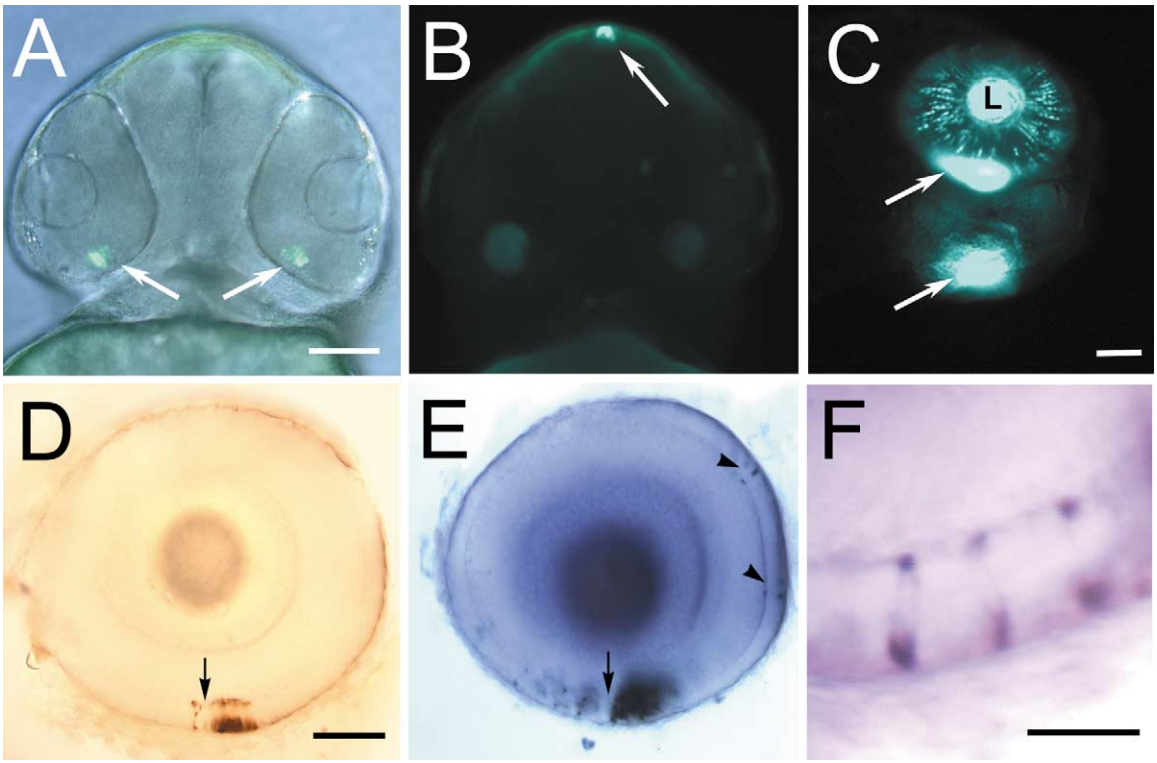


Fig. 1. Comparison of EGFP and rhodopsin expression in transgenic zebrafish. EGFP expression in photoreceptor cells (arrows) of the ventral retina (A) and the pineal (B) of transgenic zebrafish larva observed at 60 hpf. (C) At 84 hpf, EGFP fluorescence could be observed in the ventral patch (arrows) of the retinas and in cells sporadically positioned across the retina. Apparent fluorescence by the lens (L) is due to photoreceptor cell expression. *In situ* hybridization of EGFP (D) and rhodopsin (E) demonstrate a similar pattern of labeling of cells in the outer nuclear layer (ONL) of the ventral retina and on opposite sides of the choroid fissure (arrow). Sporadic labeling of cells in the ONL is also observed with the opsin probe (arrowheads). (F) Double labeling demonstrated colocalization of the EGFP transcript (brown) and rhodopsin transcript (purple) to sporadically spaced cells located in the outer nuclear layer of larval fish. Bar, 50 mm in (A–C); 25 mm in (D, E); 10 mm in (E).

However, the intensity of fluorescence and number of EGFP-expressing cells varied considerably between animals, and the pineal expression was not detected beyond larval stages. From these data, it was concluded that the *Xenopus* opsin promoter faithfully drives the expression of EGFP in rod photoreceptors of the zebrafish with occasional expression in the pineal photoreceptors.

*Rod mosaic in adult zebrafish*

When viewed under a stereoscope equipped for epifluorescence, EGFP fluorescence was readily visible in living adult zebrafish as brilliant green light emanating from the retina through the lens. To determine the distribution and architecture of the rods in the transgenic line, retinas from 3- to 6-month-old adult zebrafish were flat mounted in buffered-salt solution and analyzed by confocal microscopy (Fig. 2). Images were taken both parallel to the retinal margin and from the vitread surface through the inner layers of the retina. At a low power magnification, EGFP fluorescence was observed across the entire retina (Fig. 2A). In images taken at a higher magnification and parallel to the retinal margin, robust expression of EGFP was observed exclusively in cells with the characteristic rod morphology (Fig. 2B). In the outer plexiform layer, EGFP fluorescence was restricted to small round nerve terminals, with a single invaginating synapse and short telodendria. Each terminal was connected to a cell body by a thin axon. Distal to the densely packed cell bodies, long tapering myoids projected to the classic rod-shaped outer segments, and at the base of the outer segments, the mitochondria within the ellipsoids appeared to exclude the EGFP giving a negative profile in the fluorescent image. No clumping of the rods or gaps in their distribution was evident, suggesting that all rods were clearly labeled.

Scanning from the vitreal surface through the inner layers of the retina revealed a striking regular arrangement of the rod photoreceptors (Fig. 2C–E). In the outer plexiform layer, the pattern was characterized by regularly spaced rows of rod terminals parallel to the annular growth at the retinal margin (Fig. 2E). Distal to the densely packed cell bodies (Fig. 2D), the rod myoids projected in a reiterated pattern that spanned across the retina for distances of hundreds of micrometers (Fig. 2C). The arrangement of neighboring myoids ranged from a square to mirror image chevrons depending upon the plane of sectioning. To conform to

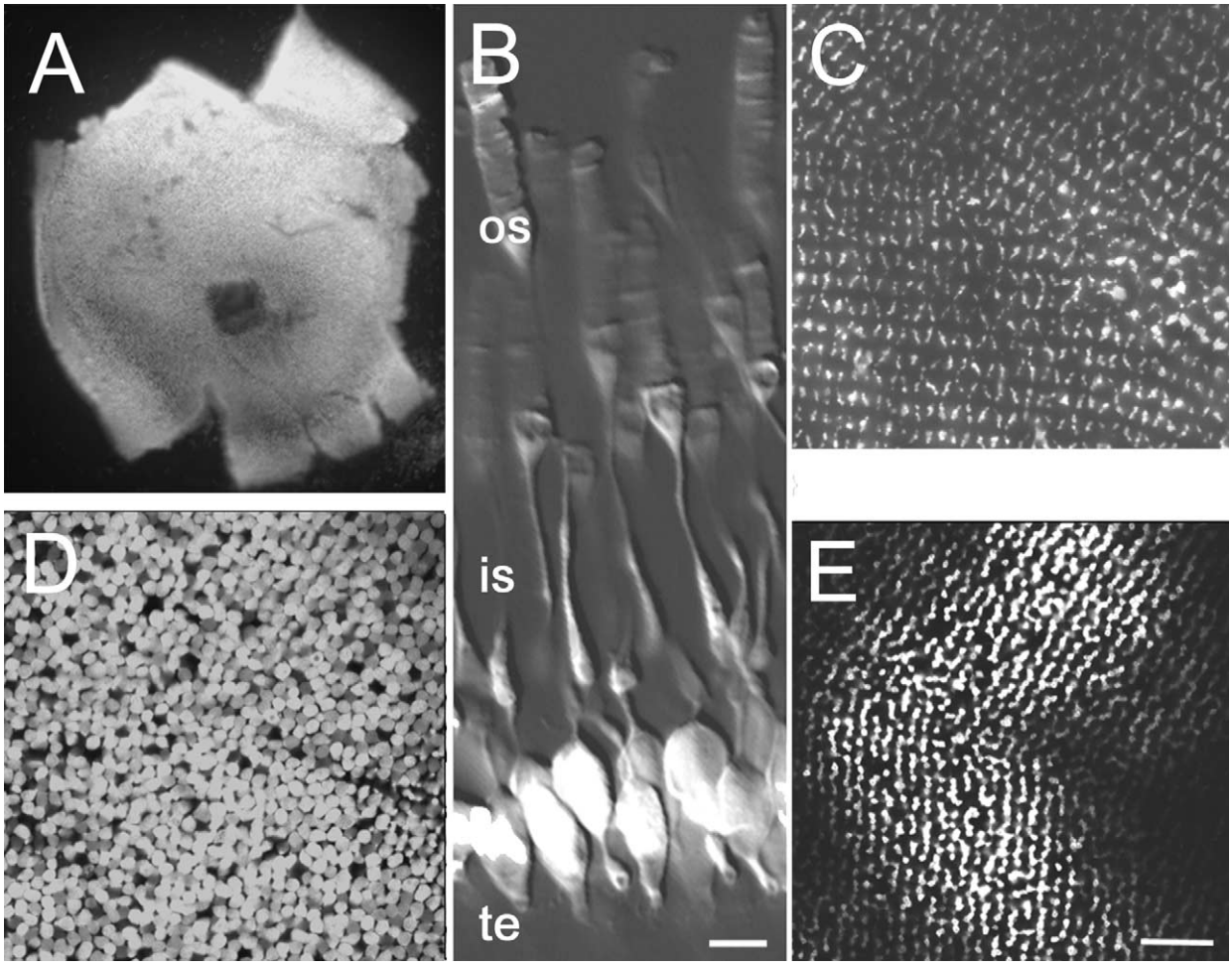


Fig. 2. Confocal analysis of EGFP expression of rod photoreceptors. Whole retinas maintained in saline were examined by confocal microscopy. (A) Low magnification image of the whole explant demonstrated robust expression of EGFP across the entire retina. (B) A higher magnification composite image of scans taken near the retinal margin. Cells with a characteristic rod morphology highlighted by small terminals (te), round soma, long thin inner segments (is), and rod-shaped outer segments (os) were observed. Images taken through the ganglion cell layer and tangential to the surface of the eye reveal a distinct organization of the rod photoreceptors at the level of the inner segments (C), cell bodies (D), and terminals (E). Note that, in each image, the rod structures are positioned in regularly spaced rows and a seam where two planes of the mosaic merge. Bar, 5 mm in (B); 20 mm in (C–E).

the curvature of the orb of the eye, the major perturbations of the regular arrangement were observed where two or more planes of the mosaic converged at acute angles. At these junctions, there was no obvious pattern underlying the arrangement of the rods. Tracking the positions of the terminals, cell bodies, and inner segments of the rods through optical sections demonstrated that they remained in register along the length of the rod; that is, they maintained their position relative to the neighboring rods, and the ellipsoids and outer segments of rods within the same square pattern converged in a cluster.

The confocal images suggested topographical organization along most of the length of the rod photoreceptor. Immunolabeling for the cone opsins and DAPI counter staining were used to accurately assign the position of the rods relative to the cone mosaic. In this and all subsequent immunolabeling, the robust EGFP fluorescence was maintained following fixation and histological processing; therefore, amplification of the EGFP signal was unnecessary. In transverse sections, expression of EGFP was observed across the entire outer layer of the retina (Fig. 3). The terminals were arranged in a single row in the outer plexiform layer, while the rod cell bodies formed a layer several nuclei in thickness. The rod myoids projected between the cones and outlined the position of the short single cones (Fig. 3A and B). A higher intensity of EGFP fluorescence was observed in the dorsal and temporal regions compared with the ventral and nasal regions, respectively. Counting the number of cells double labeled for EGFP and DAPI, this difference in fluorescence was attributed to a greater density of rods in the dorsal retina.

In tangential sections taken at the level of the short single cone outer segment, a mosaic organization of the rod myoids was apparent. The rod myoids were arranged in

squares, and the squares were arranged in parallel rows that extended toward the margin (Fig. 3A). Immunolabeling for the cone opsins identified the ultraviolet-sensitive, short single cone at the center of each rod square (Fig. 3B). DAPI counterstaining was used to label nuclei of the long single cones and the double cones. The blue cone nuclei alternated in the rows with the UV cones and rods. The nuclei of double cones ran parallel to the squares (Fig. 3C and D). Consistent with the confocal images, in sections through the distal retina, the rods formed clusters at the tip of the tapering short single cones, and in histological sections through the outer plexiform layer, the rod terminals were arranged in the parallel rows (data not shown). The mosaic pattern was best observed in younger animals and in the ventral retina where rod density was lower. In the central retina of older adults (>9 months of age), dorsal to the optic nerve, where the highest rod density was observed, the square pattern of the myoids was replaced by rows of myoids projecting between the rows of cones as previously observed (Larison and Bremiller, 1990).

*Formation of the rod mosaic*

Two mechanisms for the formation of the rod mosaic in the adult can be postulated. First, the steady though irregular proliferation of the rod progenitors and repositioning of the daughter cells could have contributed to a gradual accumulation of rods into the mosaic pattern. Alternatively, the neurogenesis near the retinal margin may have initially established the rod mosaic while ensuing proliferation across the retina simply followed the preexisting pattern. To distinguish between these two possibilities, the differentiation of the rods at the retinal margin was compared with the orderly differentiation of the cones. Immunolabeling for the cone opsins was conducted on serial sections taken near the retinal margin and oblique to the annular growth. The oblique sections give the appearance of stretching the time frame of neurogenesis when compared with the traditional transverse section.

A previous study of goldfish suggested a temporal sequence in the appearance of opsin at the retinal margin (Wan and Stenkamp, 2000). In this report, immunolabeling for the cone opsins and rhodopsin demonstrated a similar temporal sequence of expression in the zebrafish. Labeling for the red opsin was nearest to the margin, adjacent to the region of tiering of photoreceptor cell nuclei, while the initial detection of the UV opsin was observed furthest from the margin. The regular spacing of the labeled cones across the section was consistent with the mosaic organization. Immunolabeling for rod opsin was first observed in the proximity of the red cones and nearer to the margin than the first immunolabeled UV cones (data not shown). The combination of EGFP fluorescence and immunolabeling for rhodopsin revealed that, unlike the individual cones that displayed regular spacing, the rod inner and outer segments formed clusters, and that the clusters were spaced at regular intervals across the outer retina (Fig. 4A–C). Prior to any indication of tiering of the photoreceptor cell nuclei, a single immunolabeled rod marked the start of the pattern. As tiering of the photoreceptor cell nuclei became more pronounced and the rod cell bodies became aligned in a single layer just vitread to the cone nuclei, the clustering of rod myoids and outer segments became more prominent. Together, EGFP fluorescence, immunolabeling with a rod-specific monoclonal antibody, and counterstaining with DAPI revealed that the rod myoids projected apically around a cone nucleus and coalesced at a position above this centrally located cell. Immunolabeling of serial sections for the cone opsins identified the UV-cone in the central position amongst the clustered rod inner and outer segments, whereas the red and green cones alternated in position with respect the rod clusters (Fig. 4D–F). At progressively older regions of the retina (away from the margin), the rod myoids lengthened, and the space between the myoids was matched by increased length of the short single cone outer segments (compare with Fig. 3A). These data unambiguously support the alternative hypothesis that, in the adult, the rod mosaic was established at the retinal margin, and the rods form an integral component of the photoreceptor mosaic.

The identification of the orderly differentiation of rods at the margin is in stark contrast to the sporadic pattern observed in the larva. To reconcile these differences, eyes from transgenic *albino* larvae ranging from 4 to 21 dpf were imaged by confocal microscopy, and spatial analyses were applied to the data sets to determine whether the rod photoreceptor cells were randomly arranged or followed a distinct pattern. Prior to 4 dpf, the number of rods across the central retina was too sparse to facilitate spatial pattern analysis. However, between 4 and 10 dpf, after the regular arrangement of cones was well established (Fig. 5C), the number of rods dramatically increased permitting spatial analysis (Fig. 6A).

Confocal microscopy revealed that, between 4 and 10 dpf, the morphology of the EGFP expressing rods demonstrated considerable variation, with some rods displaying the classic rod morphology while others did not possessed identifiable outer segment or lacked a well-defined axon and terminal. Therefore, to avoid underestimating the number and position of the rods at these earlier stages, analyses were based on the position of the cell body. By 21 dpf, with the continued thickening of the outer layers of the retina, the positions of the terminals and cell bodies, and inner segments were clearly defined; therefore, analyses were preformed independently on both. From confocal images of the central retina, NNDs were calculated for EGFP-expressing photoreceptors, and the distribution of the cells was compared with that of a random population. For all samples analyzed, conformity ratios (NND divided by SD) revealed that the distributions of the rods were significantly different from random based on Cook's criteria (Fig. 6A; $P \leq 0.001$).

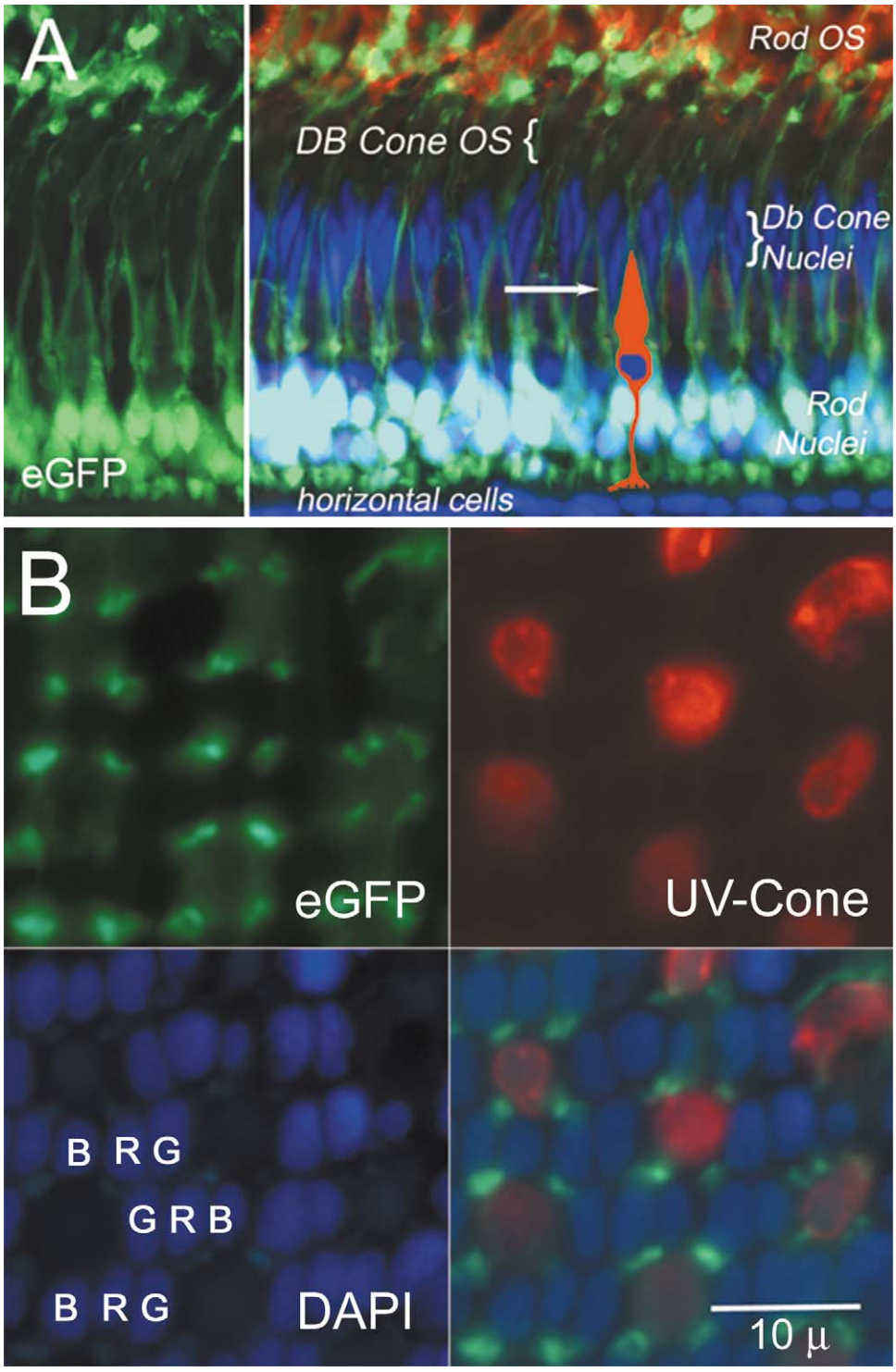


Fig. 3. Comparison of the rod mosaic to cone mosaic. (A) Transverse section through the adult retina demonstrating EGFP fluorescence in rod photoreceptors (left panel in green) and counterstaining with DAPI (blue) to reveal the tiering of the cone nuclei (left merged image). The rod cell bodies appear white due to double labeling for EGFP and DAPI. The rod outer segments are also immunolabeled for opsin. The position of the short single cone is diagrammatically represented and the plane of section in (B) is indicated by the arrow. (B) EGFP fluorescence of the rods, immunolabeling of the UV sensitive opsin, DAPI labeling of the cone nuclei in a tangential section of the adult retina and the merged image. Note the regular arrangement of the rod myoids around the outer segment of the UV-cone outer segments. (B, blue cone; G, green cone; R, red cone).

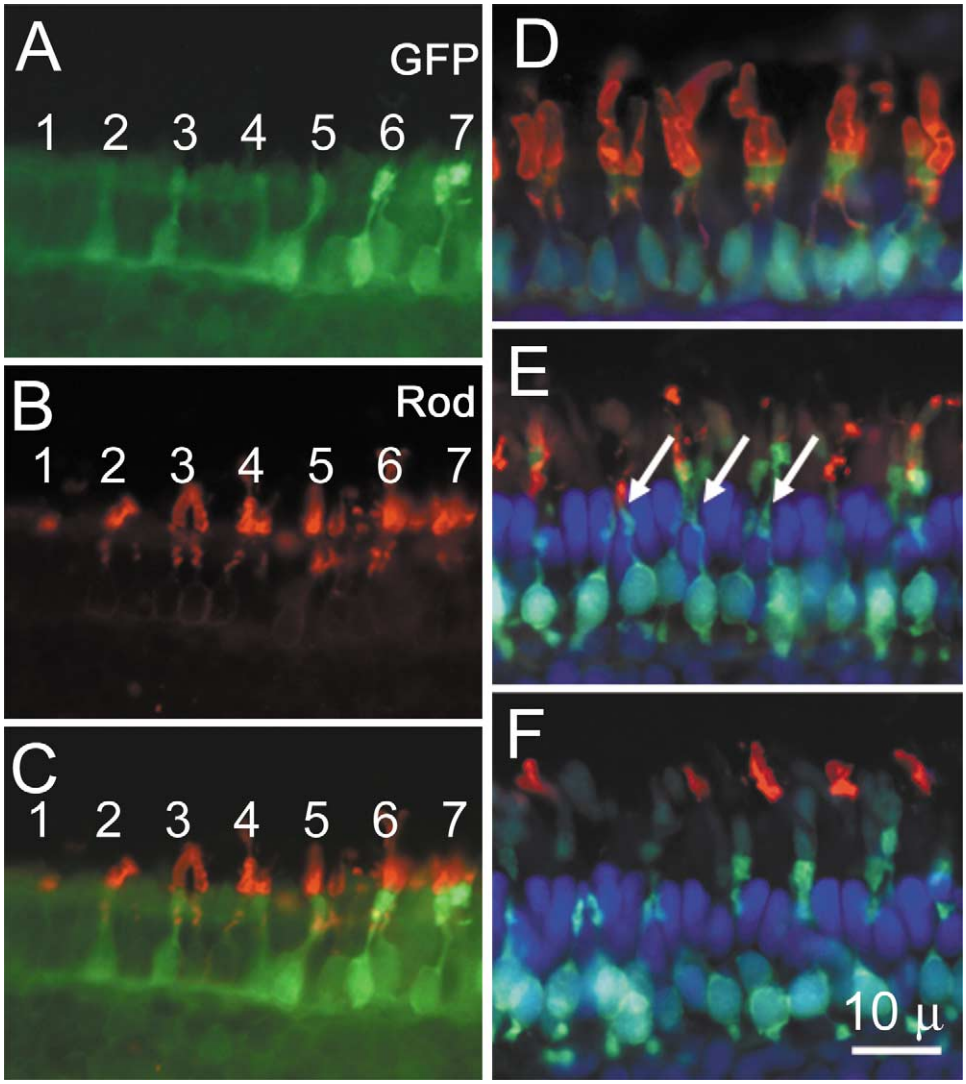


Fig. 4. Rod differentiation at the retinal margin. (A–C) EGFP expression, immunolabeling for rhodopsin (Rod), and the merged image of an oblique section through the retinal margin reveal regularly spaced clusters of rods (numbered 1–7). (D–F) Merged images of immunolabeling (red) for rhodopsin (D), UV opsin (E), and red opsin (F) with EGFP expression (green) and DAPI nuclear staining (blue) of serial sections taken parallel to the retinal margin. Note the positions of the clustered rod outer segments at the positions of the immature UV cone outer segments (arrows).

Also suggested by the quantitative analysis was that between 4 and 8 dpf, the number of rods tended to increase, and this increase correlated with the decrease in the NND (correlation coefficient, $r = -0.78$; Fig. 6B). At 21 dpf, when discrete laminae containing the rod terminals and the myoids were resolved, quantitative analysis demonstrated that their arrangements were also significantly different from random. And in the adult, where the square arrangement of the myoids was observed (Fig. 3), an even greater tendency toward nonrandomness was demonstrated (Fig. 6A).

Following spatial analysis, projections of the confocal images in three dimensions were visually inspected to determine whether the increased probability of a nonrandom arrangement of the rods in the older larvae corresponded to meaningful changes in the appearance of the mosaic. As previously reported, in embryonic and early larval stages rods appear to be sporadically arranged with the occasional arrangement of three in a row (Raymond et al., 1995). However, by 10 dpf and clearly by 21 dpf, many of the rows were arranged in parallel, thereby establishing the early square mosaic (Fig. 5B and D). But still at 21 dpf, the mosaic continued to be interrupted by gaps where one or more rods appeared to be missing. The regularity of the arrangement and the gradual appearance of the rods in parallel rows is consistent with the hypothesis that the slow proliferation of the rod progenitor cells and the directed migration of the daughter cells gradually filled the spaces between the earlier differentiated rods to generate the mosaic.

Associated with the increased regularity of the rod mosaic were changes in the morphology of the telodendria, the

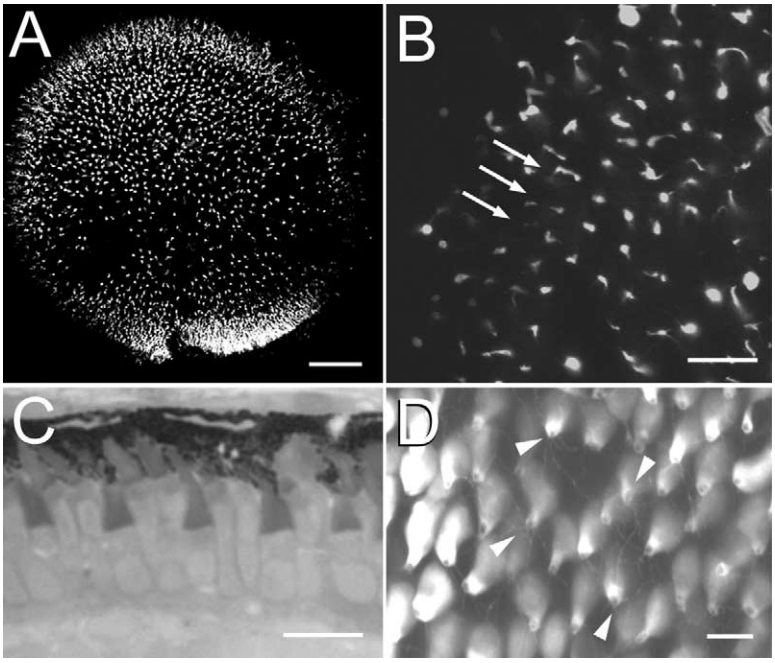


Fig. 5. Rod photoreceptor mosaic development in the larval retina. (A) Merged stack of low magnification confocal images of EGFP expression in the eye from a 10-dpf larval fish. The fluorescence appears scattered with regions of high density and obvious gaps in the distribution of rods. (B) At a higher magnification, the regular arrangement of parallel row of rods is indicated (arrows). (C) Histological section to demonstrate the regular spacing of the short single cones and the double cones in the larval retina. (D) Confocal image of EGFP fluorescence in larva 21 dpf. Note the regular arrangement of rows and the numerous telodendria extending from the rod terminals (arrowheads) Bars, 50 $\mu$m (A), 10 $\mu$m (B), 7 $\mu$m (C, D).

thin cytoplasmic extensions coupling the rod terminals. In 1-week-old larval, the telodendria spanned upwards of 20 $\mu$m to the distant rod terminals. In older larvae, the length of the telodendria and the tortuous routes consistently decreased (Fig. 5D). However, in regions where the rod mosaic was incomplete, the telodendria appeared to span across the gaps to the next closest terminals. These data suggested some degree of plasticity in the coupling of rods in the teleost retina.

## Discussion

In this report, the initial description of the rod photoreceptor mosaic in the zebrafish and the development of the pattern in the larva and adult have been presented. The data demonstrate for the first time that the positions of the rod terminals, cell bodies, and inner and outer segments are regularly arranged within the photoreceptor cell layer. Furthermore, the data show that, in the adult retina, the pattern of the mosaic is established near the retinal margin where clusters of differentiating rods were closely associated with the differentiating UV cones. By comparison, in the larva, the sporadic differentiation of rods gradually led to their accumulation in a regular pattern. The formation of the rod mosaic in the larval retina and at the margin of the adult was proceeded by the differentiation of the cones, suggesting a similar underlying mechanism to pattern the rod mosaic, whereas the variation was likely due to different rates of rods genesis.

Identification of the mosaic was in part possible because of the generation of a line of transgenic zebrafish demonstrating rod-specific expression of EGFP. Immunolabeling and in situ hybridization confirmed that the 5.5 kb of upstream sequence of the *Xenopus* opsin gene was sufficient for the robust and cell-specific expression of EGFP in the rod photoreceptors and the pineal. The pattern of expression suggests conservation across species of *trans*-acting factors and *cis*-acting elements within the rhodopsin promoter (Hamaoka et al., 2002; Knox et al., 1998; Moritz et al., 1999). Alignment of the zebrafish rhodopsin gene sequence and the *Xenopus* sequence identified a number of conserved *cis*-elements, such as Ret-1/PCE-1, OTX-1, NRE, and others implicated in retinal-specific expression (Kennedy et al., 2001; Mani et al., 2001). Interestingly, two other transgenic lines with approximately 1.2 kb of proximal sequence from either the zebrafish or *Xenopus* driving EGFP were characterized by a considerable delay in expression of the reporter gene. In the ventral patch, EGFP expression was not detected until 4–5 dpf, although at this stage, rhodopsin expression could be detected throughout the retina (Kennedy et al., 2001; Perkins et al., 2002). However, in a third report, the patterns of EGFP expression in several independent transgenic lines closely matched the spatial and temporal

**A** **Nearest Neighbor Distances and Conformity Ratios**

| Sample | NND mean (μm), ± SD (*n*)[1] | Conformity Ratio (mean/SD)[2] |
|---|---|---|
| 4 dpf | 9.48 ± 3.57 (148) | 2.66 |
| 5 dpf | 9.58 ± 3.07 (213) | 3.12 |
| 6 dpf | 8.86 ± 2.84 (234) | 3.12 |
| 7 dpf | 7.83 ± 2.17 (274) | 3.60 |
| 8 dpf | 7.32 ± 2.14 (247) | 3.42 |
| 10 dpf[3] | 7.44 ± 2.17 (538) | 3.43 |
| 21 dpf, myoid | 5.66 ± 1.41 (172) | 4.01 |
| 21 dpf, terminal | 5.10 ± 1.50 (119) | 3.34 |
| adult, myoid | 4.63 ± 1.12 (244) | 4.12 |

[1] NND and SD for a representative sample from a minimum of 3 specimen analyzed for a given stage.
[2] Statistically significant non-random patterns ($P \leq 0.001$) following criterion levels from Figure 2 of Cook (1996).
[3] Data shown in Figure 5A.

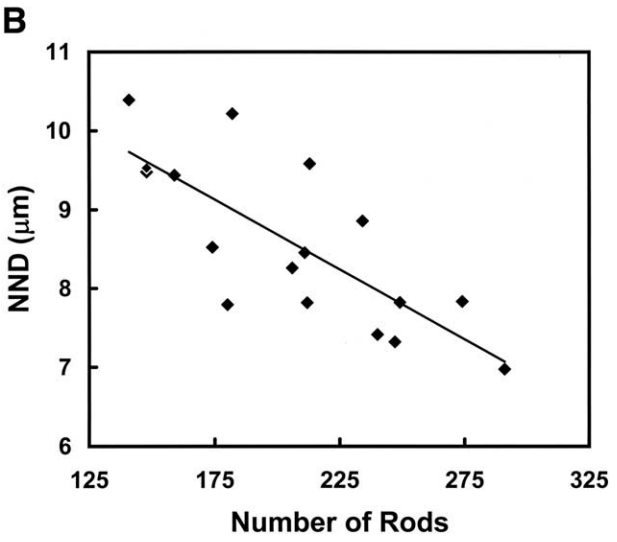


Fig. 6. Spatial pattern analysis of the rod mosaic. (A) Nearest neighbor distances (NND) and conformity ratios (CR) for a representative sample for each age of analysis. For samples between 4 and 10 dpf, the data represent distances between cell bodies. At 21 dpf and the adult, analysis based on the locations of the myoids or terminals were performed. Note the general decline in the NND and the increase in the CR as the age of the specimen increases. (B) Plot of the NND as a function of the total number of rods analyzed for larva from 4 to 8 dpf. Note the strong inverse relationship between the cell number and NND ($r = -0.78$).

pattern of rhodopsin expression. These suggest that the differences in expression observed between lines were likely due to positional effects conferred by the genomic sequences flanking the site of insertion and not the requirement of additional upstream *cis*-elements in the promoter (Hamaoka et al., 2002).

In larval and adult teleosts, rods are generated by mitosis of a population of progenitors located in the inner nuclear layer (Hagedorn and Fernald, 1992; Johns and Fernald, 1981; Julian et al., 1998; Marcus et al., 1999; Ottenson et al., 2001). Following an initial burst of mitotic activity near the retina margin, rods continue to accumulate across the retina through the proliferation of the progenitors. The potential of the rod progenitors has been extensively studied. Following experimental manipulations that damage the retina, the progenitors function as stem cells, retaining the capacity to generate most classes of retinal neurons (Raymond et al., 1988). Even following the selective ablation of cones, the progenitors demonstrated the capacity to respond and generate a small subset of the population of cells (Wu et al., 2001). However, the cells of the regenerated retinas, although functional, do not demonstrate the spatial arrangements of the native retina, suggesting that important, developmentally regulated signals are not present or not spatially regulated following injury (Cameron and Carney, 2000; Stenkamp et al., 2001; Stenkamp and Cameron, 2002).

Given the rapidly growing interest in the zebrafish as a model organism, the discovery of the rod mosaic was most surprising. Numerous studies have specifically addressed the genetic and anatomical basis of photoreceptor development and the spatial and temporal patterns of photoreceptor cell gene expression in the zebrafish, but none has conclusively demonstrated a regular pattern to the rods (Doerre and Malicki, 2001, 2002; Hyatt et al., 1996; Raymond et al., 1995; Schmitt and Dowling, 1999; Stenkamp et al., 2001). Two things may have contributed to our lack of recognition of a rod mosaic. First, limitations of the more commonly used methods of immunolabeling and in situ hybridization would have made detection of the mosaic difficult. The opsin transcript and the rhodopsin protein are vectorially sorted. This results in asymmetric labeling of the outer segment and ellipsoid, respectively (Raymond et al., 1993; Stenkamp et al., 1997). The dense packing of the ellipsoids and outer segments further obscured the mosaic by limiting the ability to resolve individual structures. Second, for numerous reasons, most studies restricted analysis of retinal development to 5 dpf. At this stage, the number of rods was still comparatively low and the arrangement still appeared sporadic. Although the occasional or coincidental arrangement of 3 rods in a row had been reported (Raymond et al., 1995), it was not until 9 or 10 dpf that a two-dimensional arrangement was observed. Although spatial pattern analysis has been successfully used to test the arrangement of numerous cells in the adult retina and the pattern of amacrine cells in the developing mammalian retina (Cook and Chalupa, 2000; Galli-Resta, 2000; Stenkamp and Cameron, 2002), prior to this study, it had not been used in the systematic analysis of photoreceptor cell development in the larval teleost. Thus the identification of the rod mosaic benefited from both transgenic technologies to label specific cells and advances in imaging and analysis techniques.

In retrospect, a mosaic pattern to the rods should not

have been unexpected. A regular pattern could optimize packing density, maximize photon absorption, or direct incorporation of newly differentiated rods into the appropriate retinal circuitry. Based on electron microscopy, a regular arrangement of the rod myoids projecting through the cone mosaic had been reported in the developing guppy (*Poecilia reticulata*) and cichlid (*Nannacara anomala*); therefore, a similar arrangement to the outer segments in zebrafish was not without precedent (Kunz et al., 1983; Ali et al., 1978). However, in the guppy, the embryonic pattern was rapidly replaced by the random projection of the rods through the cone mosaic. Furthermore, neither study described the spatial and temporal pattern of rod genesis at the margin or a pattern associated with the rod terminals. In the larval goldfish, quantitative analysis demonstrated a rod to cone ratio of approximately 1:1 (Johns, 1982), and in the larval zebrafish, equal numbers of rod and UV cones were reported (Doerre and Malicki, 2001, 2002). Although in the goldfish this rod:cone ratio was also quickly overshadowed by the rapid recruitment of additional rods across the retina (Johns, 1982), their presence suggests conservation of an underlying mechanism to initially establish a relationship between the differentiating rods and the other neuronal population. Serial reconstruction of electron micrographs to establish such a relationship would be a daunting proposition, whereas EGFP expression in conjunction with confocal microscopy made spatial analysis comparatively easy. Ideally, future studies would not be limited to spatial analysis but would combine the expression of fluorescent reporter genes with recent advances in multiphoton microscopy to investigate the migration, differentiation, and morphogenesis of cells in vivo. The current limitation of such studies is the availability of transgenic lines demonstrating cell or tissue specific expression of fluorescent reporter genes.

Based on the precocious expression of rhodopsin in the ventral patch, it had been proposed that rods influence cone mosaic formation. However, a subsequent study of photoreceptor cell differentiation near the retinal margin discounted the role of rods in the arrangement of the cones (Wan and Stenkamp, 2000). The present data not only support the later but also extend the findings to enable us to draw the conclusion that the cones influence the mosaic organization of the rods. Although it has been well documented that diffusible factors, such as retinoic acid and members of the sonic hedgehog gene family, promoted the differentiation of rods (Hyatt et al., 1996; Stenkamp et al., 2000), the presence of a rod mosaic suggests that local cell-to-cell interactions are also important. Therefore, a two-stage model for the formation and maintenance of the rod mosaic is proposed. As postmitotic cells migrate into the outer nuclear layer, their spatial position within the photoreceptor cell mosaic is guided by local cell-to-cell interactions. Initially, homotypic cell-to-cell interactions between the postmitotic cells and differentiated rods would induce tangential migration of the postmitotic cells to ensure regular spacing of the rods within the photoreceptor cell layer, similar to mechanisms proposed for the mosaic organization of other retinal neurons (Cook and Chalupa, 2000; Galli-Resta, 2000). In the second step, during morphogenesis, heterotypic cell-to-cell interactions between the postmitotic cells and the neighboring cones and possibly bipolar cells direct the alignment of the rod terminals and the inner and outer segments within the existing neural circuitry. As new rods are generated across the central retina, they follow the cues provided by the existing mosaic, leading to multiple rods at each corner position around the UV cones.

An alternative hypothesis for formation of the rod mosaic would propose that migrating rods are not guided by cell-to-cell interactions, but rather, are merely taking the path of least resistance. Although this cannot be completely ruled out, relying solely on a passive mechanism is unlikely considering the current data. Tangential dispersion of the postmitotic cells is necessary to ensure a nonrandom arrangement of rods in the larva. Likewise, dispersion would initiate the arrangement of the rod inner and outer segments within the cone mosaic at the retinal margin. Without such a mechanism, a random arrangement of the rod cell bodies in the larva or clumping of the inner segments within the photoreceptor cell layer would have been detected by the spatial analysis. It is possible that, at the retinal margin, a selective adhesion between the red and green sensitive members of the double cones in part excludes the rods from the intervening space. As a result, the rods become confined to the extracellular space between the UV- and blue-sensitive cones. However, mechanisms to ensure nonrandom spacing of the rod terminals and an even distribution of the inner segments around the UV-cone would still be necessary.

This clear separation of phenotypic maturation from positional information is supported by the phenotypes of several mutations that affect retinal lamination in zebrafish (Jensen et al., 2001; Malicki and Driever, 1999). In several of these mutants, phenotypic differentiation of neurons, monitored by cell-specific gene expression, continues although discrete nuclear and plexiform layers do not form. For example, the photoreceptor cells of *mosaic eyes* do not form a distinct lamina (Jensen et al., 2001). Whereas the cones were arranged in distinct layers in both the outer and inner layers of the retina, cells expressing rhodopsin were distributed across the central retina. In *oko meduzy*, another mutation affecting retinal lamination, rod and cone opsins could be detected in cells with no apparent organization (Malicki and Driever, 1999). These data would suggest that expression of a rod cell phenotype (opsin expression) was independent of positional information provided by the cone photoreceptors. Unfortunately, direct genetic evidence that rods can differentiate in the complete absence of cones or that cones direct the patterning of the rods within the mosaic is not available. Of the numerous mutations that alter photoreceptor cell development and survival, most result in

nonspecific alterations of all photoreceptors (Doerre and Malicki, 2001, 2002; Fadool et al., 1997). To support the proposed heterotypic interactions between rods and cones, mutations that specifically alter the stages of rod maturation and patterning of the photoreceptor cell mosaic need to be identified. Therefore, a highly focused screen to identify loci that alter the spatial and temporal pattern of EGFP expression in this transgenic line is warranted.

The diffusion of the soluble form of EGFP throughout the cytoplasm allowed unambiguous identification of rod structures, their organization into a mosaic, and the patterning of the mosaic across the retina. For example, the rod terminals with the characteristic single invaginating synapse were easily resolved, and the numerous, thin telodendria extending from the terminals were readily detected although their dimensions are near the limit of resolution for fluorescence microscopy. The rod–rod junctions are an adaptation, more commonly reported in amphibian and reptilian retinas, postulated to reduce electrical noise associated with the thermal isomerization of rhodopsin (Witkovsky et al., 2001). In teleosts, rod–cone junctions are usually observed, and like their mammalian counterparts, may function to couple rods to the more elaborate circuitry of the cone pathway (Kolb et al., 2001). Although direct evidence of rod–cone coupling was not observed, the presence of en passant contact, as the telodendria looped through the outer plexiform layer, could not be excluded.

The regular arrangement of the rod terminals, and hence the synaptic connections, suggests a tightly regulated molecular mechanism for integrating the rods into the existing retinal circuitry. In the carp, differentiating rods establish the appropriate synaptic connections with preexisting second order neurons and the same is thought to be true in zebrafish. As the number of rods increased, the number of synapses onto the rod bipolar cells also increased (Kock and Stell, 1985). However, from the data, it was not possible to determine whether synapse formation is limited to available sites on the bipolar cells or if the projection of the rod axon is restricted to locations defined by other cellular elements such as the large cone terminals. In this broader context, the intensely studied rod progenitors combined with the genetic capabilities in zebrafish should provide a tractable model of stem cell biology, more specifically, to identify the molecular mechanisms essential for the precise incorporation of the newly generated neurons into a preexisting neural network.

## Acknowledgments

This work was supported by NIH Grant EY13020 and a First Year Assistant Professor Award from FSU. The author wishes to thank D.R. Hyde and T.S. Vihtelic for polyclonal antisera against the cone opsins, B. Knox and D. Papermaster for *Xenopus* opsin promoter-EGFP plasmids, and the staff of the Biological Science Imaging Resources Facility.

## References

Ali, M.A., 1976. Retinas of Fishes: An Atlas. Springer-Verlag, New York.

Ali, M.A., Harosi, F.I., Wagner, H.J., 1978. Photoreceptors and visual pigments in a cichlid fish, Nannacara anomala.. Sens. Processes 2, 130–145.

Cameron, D.A., Carney, L.H., 2000. Cell mosaic patterns in the native and regenerated inner retina of zebrafish: implications for retinal assembly. J. Comp. Neurol. 416, 356–367.

Cook, J.E., Chalupa, L.M., 2000. Retinal mosaics: new insights into an old concept. Trends Neurosci. 23, 26–33.

Doerre, G., Malicki, J., 2001. A mutation of early photoreceptor development, mikre oko, reveals cell- cell interactions involved in the survival and differentiation of zebrafish photoreceptors. J. Neurosci. 21, 6745–6757.

Doerre, G., Malicki, J., 2002. Genetic analysis of photoreceptor cell development in the zebrafish retina. Mech. Dev. 110, 125–138.

Engstrom, K., 1960. Cone types and cone arrangements in retina of some cyprinids. Acta Zool. (Stockholm) 41, 277–295.

Fadool, J.M., Brockerhoff, S.E., Hyatt, G.A., Dowling, J.E., 1997. Mutations affecting eye morphology in the developing zebrafish (Danio rerio). Dev. Genet. 20, 288–295.

Fernald, R.D., 1990. Teleost vision: seeing while growing. J. Exp. Zool. (Suppl. 5), 167–180.

Galli-Resta, L., 2000. Local, possibly contact-mediated signaling restricted to homotypic neurons controls the regular spacing of cells within the cholinergic arrays in the developing rodent retina. Development 127, 1509–1516.

Hagedorn, M., Fernald, R.D., 1992. Retinal growth and cell addition during embryogenesis in the teleost, Haplochromis burtoni. J. Comp. Neurol. 321, 193–208.

Hagedorn, M., Mack, A.F., Evans, B., Fernald, R.D., 1998. The embryogenesis of rod photoreceptors in the teleost fish retina, Haplochromis burtoni. Brain Res. Dev. Brain Res. 108, 217–227.

Hamaoka, T., Takechi, M., Chinen, A., Nishiwaki, Y., Kawamura, S., 2002. Visualization of rod photoreceptor development using GFP-transgenic zebrafish. Genesis 34, 215–220.

Hu, M., Easter, S.S., 1999. Retinal neurogenesis: The formation of the initial central patch of postmitotic cells. Dev. Biol. 207, 309–321.

Hyatt, G.A., Schmitt, E.A., Fadool, J.M., Dowling, J.E., 1996. Retinoic acid alters photoreceptor development in vivo. Proc. Natl. Acad. Sci. USA 93, 13298–13303.

Jensen, A.M., Walker, C., Westerfield, M., 2001. *mosaic eyes*: a zebrafish gene required in the pigmented epithelium for apical localization of retinal cell division and lamination. Development 128, 95–105.

Johns, P.R., Fernald, R.D., 1981. Genesis of rods in teleost fish retina. Nature 293, 141–142.

Johns, P.R., 1982. Formation of photoreceptors in larval and adult goldfish. J. Neurosci. 2, 178–198.

Julian, D., Ennis, K., Korenbrot, J.L., 1998. Birth and fate of proliferative cells in the inner nuclear layer of mature fish retina. J. Comp. Neurol. 394, 271–282.

Kennedy, B.N., Vihtelic, T.S., Checkley, L., Vaughan, K.T., Hyde, D.R., 2001. Isolation of a zebrafish rod opsin promoter to generate a transgenic zebrafish line expressing enhanced green fluorescent protein in rod photoreceptors. J. Biol. Chem. 276, 14037–14043.

Knox, B.E., Schlueter, C., Sanger, B.M., Green, C.B., Besharse, J.C., 1998. Transgene expression in Xenopus rods. FEBS Lett. 423, 117–121.

Kock, J.H., Stell, W.K., 1985. Formation of new rod photoreceptor synapses onto differentiated bipolar cells in goldfish retina. Anat. Rec. 211, 69–74.

Kolb, H., Nelson, R., Ahnelt, P., Cuenca, N., 2001. Cellular organization of the vertebrate retina. Prog. Brain Res. 131, 3–26.

Kunz, Y.W., Ennis, S., Wise, C., 1983. Ontogeny of the photoreceptors in the embryonic retina of the viviparous guppy, Poecilia reticulata P. (Teleostei). An electron- microscopical study. Cell Tissue Res. 230, 469–486.

Larison, K.D., BreMiller, R., 1990. Early onset of phenotype and cell patterning in the embryonic zebrafish retina. Development 109, 567–576.

Livesey, F.J., Cepko, C.L., 2001. Vertebrate neural cell-fate determination: lessons from the retina. Nat. Rev. Neurosci. 2, 109–118.

Lohmann, C., Wong, R.O., 2001. Cell-type specific dendritic contacts between retinal ganglion cells during development. J. Neurobiol. 48, 150–162.

Malicki, J., Driever, W., 1999. oko meduzy mutations affect neuronal patterning in the zebrafish retinal and reveal cell-cell interactions in the neuroepithelial sheet. Development 126, 1235–1246.

Mani, S.S., Batni, S., Whitaker, L., Chen, S., Engbretson, G., Knox, B.E., 2001. Xenopus rhodopsin promoter. Identification of immediate upstream sequences necessary for high level, rod-specific transcription. J. Biol. Chem. 276, 36557–36565.

Marcus, R.C., Delaney, C.L., Easter Jr., S.S., 1999. Neurogenesis in the visual system of embryonic and adult zebrafish (Danio rerio). Vis. Neurosci. 16, 417–424.

Masland, R.H., Raviola, E., 2000. Confronting complexity: strategies for understanding the microcircuitry of the retina. Annu. Rev. Neurosci. 23, 249–284.

Masland, R.H., 2001. The fundamental plan of the retina. Nat. Neurosci. 4, 877–886.

Mollereau, B., Dominguez, M., Webel, R., Colley, N.J., Keung, B., de Celis, J.F., Desplan, C., 2001. Two-step process for photoreceptor formation in Drosophila. Nature 412, 911–913.

Moritz, O.L., Tam, B.M., Knox, B.E., Papermaster, D.S., 1999. Fluorescent photoreceptors of transgenic Xenopus laevis imaged in vivo by two microscopy techniques. Invest. Ophthalmol. Vis. Sci. 40, 3276–3280.

Otteson, D.C., D'Costa, A.R., Hitchcock, P.F., 2001. Putative stem cells and the lineage of rod photoreceptors in the mature retina of the goldfish. Dev. Biol. 232, 62–76.

Perkins, B.D., Kainz, P.M., O'Malley, D.M., Dowling, J.E., 2002. Transgenic expression of a GFP-rhodopsin COOH-terminal fusion protein in zebrafish rod photoreceptors. Vis. Neurosci. 19, 257–254.

Peterson, R.E., Fadool, J.M., McClintock, J., Linser, P.J., 2001. Muller cell differentiation in the zebrafish neural retina: evidence of distinct early and late stages in cell maturation. J. Comp. Neurol. 429, 530–540.

Raymond, P.A., Barthel, L.K., Curran, G.A., 1995. Developmental patterning of rod and cone photoreceptors in embryonic zebrafish. J. Comp. Neurol. 359, 537–550.

Raymond, P.A., Barthel, L.K., Rounsifer, M.E., Sullivan, S.A., Knight, J.K., 1993. Expression of rod and cone visual pigments in the goldfish and zebrafish: A rhodopsin-like gene is expressed in cones. Neuron 10, 1161–1174.

Raymond, P.A., Reifler, M.J., Rivlin, P.K., 1988. Regeneration of goldfish retina: rod precursors are a likely source of regenerated cells. J. Neurobiol. 19, 431–463.

Reese, B.E., Harvey, A.R., Tan, S.S., 1995. Radial and tangential dispersion patterns in the mouse retina are cell-class specific. Proc. Natl. Acad. Sci. USA 92, 2494–2498.

Reese, B.E., Galli-Resta, L., 2002. The role of tangential dispersion in retinal mosaic formation. Prog. Retinal Eye Res. 21, 153–168.

Rockhill, R.L., Euler, T., Masland, R.H., 2000. Spatial order within but not between types of retinal neurons. Proc. Natl. Acad. Sci. USA 97, 2303–2307.

Schmitt, E.A., Dowling, J.E., 1996. Comparison of topographical patterns of ganglion and photoreceptor cell differentiation in the retina of the zebrafish, Danio rerio. J. Comp. Neurol. 371, 222–234.

Schmitt, E.A., Dowling, J.E., 1999. Early retinal development in the zebrafish, Danio rerio: light and electron microscopic analyses. J. Comp. Neurol. 404, 515–536.

Stenkamp, D.L., Hisatomi, O., Barthel, L.K., Tokunaga, F., Raymond, P.A., 1996. Temporal expression of rod and cone opsins in embryonic goldfish retina predicts the spatial organization of the cone mosaic. Invest. Ophthalmol. Vis. Sci. 37, 363–376.

Stenkamp, D.L., Barthel, L.K., Raymond, P.A., 1997. Spatiotemporal coordination of rod and cone photoreceptor differentiation in goldfish retina. J. Comp. Neurol. 382, 272–284.

Stenkamp, D.L., Frey, R.A., Prabhudesai, S.N., Raymond, P.A., 2000. Function for Hedgehog genes in zebrafish retinal development. Dev. Biol. 220, 238–252.

Stenkamp, D.L., Powers, M.K., Carney, L.H., Cameron, D.A., 2001. Evidence for two distinct mechanisms of neurogenesis and cellular pattern formation in regenerated goldfish retinas. J. Comp. Neurol. 431, 363–381.

Stenkamp, D.L., Cameron, D.A., 2002. Cellular pattern formation in the retina: retinol regeneration as a model system. Mol. Vis. 8, 280–293.

Vihtelic, T.S., Doro, C.J., Hyde, D.R., 1999. Cloning and characterization of six zebrafish photoreceptor opsin cDNAs and immunolocalization of their corresponding proteins. Vis. Neurosci. 16, 571–585.

Wan, J., Stenkamp, D.L., 2000. Cone mosaic development in the goldfish retina is independent of rod neurogenesis and differentiation. J. Comp. Neurol. 423, 227–242.

Wassle, H., Riemann, H.J., 1978. The mosaic of nerve cells in the mammalian retina. Proc. R. Soc. Lond. B Biol. Sci. 200, 441–461.

Wassle, H., Boycott, B.B., Illing, R.B., 1981. Morphology and mosaic of on- and off-beta cells in the cat retina and some functional considerations. Proc. R. Soc. Lond. B Biol. Sci. 212, 177–195.

Witkovsky, P., Thoreson, W., Tranchina, D., 2001. Transmission at the photoreceptor synapse. Prog. Brain Res. 131, 145–159.

Wu, D.M., Schneiderman, T., Burgett, J., Gokhale, P., Barthel, L., Raymond, P.A., 2001. Cones regenerate from retinal stem cells sequestered in the inner nuclear layer of adult goldfish retina. Invest. Ophthalmol. Vis. Sci. 42, 2115–2124.